

ANALYSIS OF THREE-DIMENSIONAL SOUND RADIATION PROBLEMS USING TRIMMED PATCH BOUNDARY ELEMENTS

Christopher G. Provatidis

Laboratory of Dynamics and Mechanical Structures
National Technical University of Athens
157 73 Athens, Greece
e-mail: cprovat@central.ntua.gr

Keywords: Boundary Elements, Coons patch, Trimmed-patch, Macroelements, Helmholtz equation, Acoustics.

Abstract. *This paper investigates the performance of trimmed patch boundary elements in sound radiation problems, which are described by the Helmholtz equation. Instead of dividing the vibrating surface into a high number of boundary elements, this is transformed into a small number of four-sided patches where Coons interpolation is applied. In many cases the whole surface is mapped to six surfaces of a curvilinear paralleloid and nodal points are arranged only along the twelve sides of the paralleloid. In this way, the number of the degrees of freedom is drastically reduced by one dimension and the entire computational procedure is highly speed-up. The proposed elements are successfully applied to a vibrating cube due to a monopole.*

1 INTRODUCTION

Trim patch boundary elements were initially proposed in 1989 for stress analysis of structures [1]. Tzanakis and Provatidis [2] in 3D-elastostatics independently worked out the same idea, at the same period. This method was further extended and recently published [3]. Reference [1] was unknown to the author until quite recently a reviewer mentioned its existence during the revision of Reference [4] that refers to 2D axisymmetric elastostatics.

The main idea of the above method is general and therefore can be extended to other classes of problems such as sound radiation problems. The details are as follows. Instead of arranging the degrees of freedom along the entire boundary (local approximation), these DOF are arranged only along the edges of large patches in which the boundary is divided (global approximation). In [1] the unknown variable along a surface patch was interpolated using a *Lagrange* polynomial, which however appear numerical oscillations. Instead, *Coons-patch* interpolation is here proposed; it is very smooth especially when using B-splines [2,3] and not only.

With respect to the particular application of the Coons-patch method to sound radiation problems, it was previously shown that the direct application of the BEM leads to numerical instabilities, which are usually called “fictitious eigenvalues”. The problem is overcome using several techniques that may be found in a recent publication [5].

In this paper the proposed method is applied to a cube radiator for the case of a monopole. The degrees of freedom are arranged along the twelve edges of the cube. This technique offers a great advantage. For example, if each edge was divided into 5 nodes (4 equal segments), the proposed method requires $12 \times 3 + 8 = 44$ nodal points along the twelve sides, while the conventional BEM requires *additional* 54 nodes, that is totally $44 + (3 \times 3) \times 6 = 98$ nodal points of linear type interpolation elements. As it was the case for conventional boundary elements, reliable (stable) results were obtained when using an extra point at the centre of the cube [6].

2 GENERAL THEORY

2.1 Sound radiation formulation

In sound radiation problems the objective purpose is to solve Helmholtz equation

$$\nabla^2 p + k^2 p = 0 \quad (1)$$

where p denotes the acoustic pressure, k the wavenumber ($k = \omega/c$), ω the cyclic frequency, c the sound velocity and ∇ the Nabla operator.

The weak formulation of eq.(1) in the infinite volume V is:

$$\int_V p_i^* (\nabla^2 p + k^2 p) dV = 0 \quad (2)$$

where p_i^* is the fundamental solution given as:

$$p_i^* = e^{-jkR} / (4\pi R) \quad (3)$$

with R denoting the Euclidian distance between the *source* point ' i ' and the *field* one.

Then, by applying Green's theorem on Eq (2), one obtains the Direct-BEM-formulation:

$$c_i p_i + \oint_S p q_i^* dS = \oint_S q p_i^* dS \quad (4)$$

where

$$q = \mathbf{n} \nabla p \quad \text{and} \quad q_i^* = \frac{\partial p_i^*}{\partial \mathbf{n}} \quad (5)$$

with \mathbf{n} denoting the outward normal unit vector on the boundary S . The coefficient $c_i = 0, 1/2$ or 1 denotes an internal (in \bar{V}), a boundary (on S) or an external (in V) source point ' i ', respectively (\bar{V} =volume surrounded by the surface S , while V =exterior volume=infinite).

Particularly, the Neumann acoustic radiation problem, which is the subject of this paper, consists of the calculation of the pressure p on the surface S , which vibrates with a prescribed normal harmonic velocity \mathbf{v}_n . If \mathbf{a} is the boundary acceleration, Euler's equation relates the pressures as follows:

$$\nabla p = -\rho \mathbf{a} = -j\omega \rho \mathbf{v} \quad (6)$$

where ρ is the density of the fluid that surrounds the vibrating surface and $j^2 = -1$.

Therefore

$$q = -j\omega \rho \cdot (\mathbf{n} \cdot \mathbf{v}) = -j\omega \rho \mathbf{v}_n \quad (7)$$

It is well-known that the above Direct-BEM-formulation [eq.(4)] fails to yield unique solution at certain wavenumbers corresponding to eigenvalues of the interior Dirichlet problem of closed surface [5].

As it can be noticed, in Eq. (4) only boundary integrals are involved. The advantage of BEM is that it reduces the dimensionality of the problem by one; from 3D (volume) to 2D (surface) integrals. The common practice is to solve Eq. (4) in conjunction with constant, linear or quadratic interpolation of both the acoustic pressure p and velocity v along the boundary of the surface S .

2.2 Global approximation

In order to interpolate p and v in a more efficient way, let us assume that the surface S under consideration is made of a few large surface patches. Let us also assume that over each patch the variation of both boundary pressures and velocities is adequately smooth (not an abrupt change occurs). The novel idea of this paper is to interpolate both boundary pressures and velocities within each patch by applying a global set of cardinal functions instead of dividing all surfaces in small boundary elements. In this way, the number of degrees of freedom is drastically reduced.

The global interpolation is performed as follows. Within each patch the pressure and velocity are expressed with respect to nodal points arranged along the four surrounding edges. As a result, the nodal points and the associated degrees of freedom appear only along the edges of the boundary. So, the boundary pressure $p(x, y, z)$ inside a patch is approximated by:

$$p(\xi, \eta) = \sum_{k=1}^K \Phi_k(\xi, \eta) p_k \quad (8)$$

with $\Phi_k(\xi, \eta)$ denoting the global shape function, p_k nodal degrees of freedom appearing only at the boundaries of the patch, while ξ and η being its normalised ($0 \leq \xi, \eta \leq 1$) curvilinear co-ordinates.

Following Coons [11], the co-ordinates of a point $\mathbf{x}(\xi, \eta)$ inside a four-sided patch can be expressed in a

closed analytical form in terms of its four “boundaries” $\xi = 0, 1$ and $\eta = 0, 1$: $\mathbf{x}(0, \eta)$, $\mathbf{x}(1, \eta)$, $\mathbf{x}(\xi, 0)$, $\mathbf{x}(\xi, 1)$:

$$\begin{aligned} \mathbf{x}(\xi, \eta) = & (1-\xi) \mathbf{x}(0, \eta) + \xi \mathbf{x}(1, \eta) + (1-\eta) \mathbf{x}(\xi, 0) + \eta \mathbf{x}(\xi, 1) \\ & - (1-\xi)(1-\eta) \mathbf{x}(0, 0) - \xi(1-\eta) \mathbf{x}(1, 0) \\ & - (1-\xi)\eta \mathbf{x}(0, 1) - \xi\eta \mathbf{x}(1, 1) \end{aligned} \quad (9)$$

In this paper it is assumed that pressure p inside the patch are also implemented in a similar way, as follows:

$$p(\xi, \eta) = E_0(\xi) p(0, \eta) + E_1(\xi) p(1, \eta) + E_0(\eta) p(\xi, 0) + E_1(\eta) p(\xi, 1) - \sum_{i=0}^1 \sum_{j=0}^1 E_i(\xi) E_j(\eta) p(\xi_i, \eta_j) \quad (10)$$

The “blending” functions shown in Figure 1 ($u=p$) are given as

$$E_0(\eta) = 1 - \eta, \quad E_1(\eta) = \eta \quad (11)$$

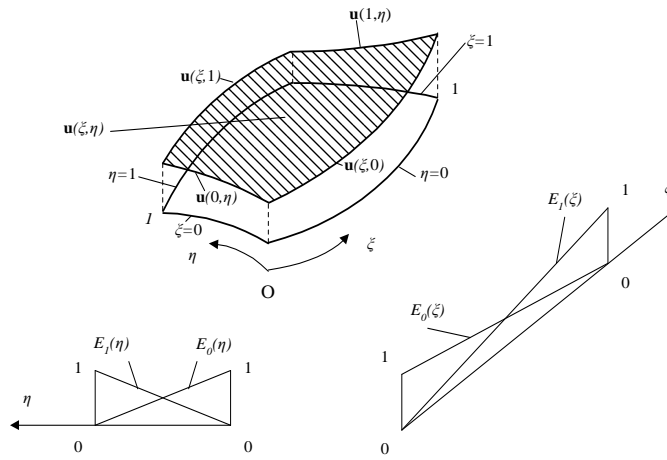


Figure 1. Boundary curves $p(0, \eta)$, $p(1, \eta)$, $p(\xi, 0)$, $p(\xi, 1)$ and ‘blending functions’ E_0 and E_1 of the patch.

Following Provatidis and Kanarachos [7], having prescribed $3q$ (different) degrees of freedom ($3q$ nodes) on each boundary, $p(0, \eta_i)$, $p(1, \eta_i)$, $p(\xi_i, 0)$, $p(\xi_i, 1)$, $i=1, 2, \dots, q$, appropriate interpolating formulae for the functions $p(0, \eta)$, $p(1, \eta)$, $p(\xi, 0)$ and $p(\xi, 1)$ are sought. Considering that q may be allowed to be a large number, a Lagrangian interpolation polynomial would tend to produce undesirable oscillations between two arbitrary abscissae η_i and η_{i+1} , as it may possess as many as $(q-1)$ maxima and minima over its entire interval of variation. For this reason, the use of splines is envisaged:

Given q degrees of freedom on the boundary of the patch at n_1, n_2, \dots, n_q a spline function $B(n)$ of degree m is a function having the two following properties:

- (1) In each interval (n_i, n_{i+1}) , $i=1, 2, \dots, q-1$, $B(n)$ is given by a polynomial of degree m or less.
- (2) $B(n)$ and its derivatives of order $1, 2, \dots, m-1$ are continuous everywhere.

A commonly used spline function is the truncated power function $\langle n - n_i \rangle^m$, for any variable $n - n_i$ and for any positive integer m . This function is defined by:

$$\begin{aligned} \langle n - n_i \rangle^m &= (n - n_i)^m, \quad \text{for } n - n_i > 0; \\ \langle n - n_i \rangle^m &= 0, \quad \text{for } n - n_i < 0 \end{aligned} \quad (12)$$

It is easily seen that the function $B(n)$ has a unique representation of the form:

$$B(n) = b_0 + b_1 n + b_2 n^2 + \dots + b_{m-1} n^{m-1} + \sum_{i=1}^{q-1} a_i \langle n - n_i \rangle^m = P(n) + \sum_{i=1}^{q-1} a_i \langle n - n_i \rangle^m \quad (13)$$

with $P(n)$ denoting a polynomial of degree $(m-1)$ and a_i properly chosen constants. The most common case is that the spline of order $m = 4$ (degree 3), that is of cubic B-splines. If now $B_j(n)$, where n is either ξ or η , denote cardinal splines of degree m , then the functions $p(0, \eta)$, $p(1, \eta)$, $p(\xi, 0)$ and $p(\xi, 1)$ could be written in the following form:

$$\begin{aligned} p(0, \eta) &= \sum_{j=1}^q B_j(\eta) p(0, \eta_j) & p(1, \eta) &= \sum_{j=1}^q B_j(\eta) p(1, \eta_j) \\ p(\xi, 0) &= \sum_{j=1}^q B_j(\xi) p(\xi_j, 0) & p(\xi, 1) &= \sum_{j=1}^q B_j(\xi) p(\xi_j, 1) \end{aligned} \quad (14)$$

which, when substituting in Eq. (10), determines the global shape functions $\Phi_k(\xi, \eta)$ involved in Eq. (8).

3 NUMERICAL IMPLEMENTATION

3.1 General procedure

The co-ordinate vector within the ip -th patch ($ip = 1, \dots, N_p$) is interpolated on the basis of the boundaries of the patch, which consists of N^{ip} nodes, as follows

$$\mathbf{x}(\xi, \eta) = \sum_{j=1}^{N^{ip}} \Phi_j(\xi, \eta) \mathbf{x}_j = \mathbf{\Phi}_{ip}^T \mathbf{x}_{ip} \quad (15)$$

It is also considered that both the pressure and velocity vectors at a point $\mathbf{P}(\xi, \eta)$ within the patch are interpolated in the same manner (isoparametric macro-element)

$$\begin{aligned} p(\xi, \eta) &= \sum_{j=1}^{N^{ip}} \Phi_j(\xi, \eta) p_j = \mathbf{\Phi}_{ip}^T \mathbf{p}_{ip} \\ v(\xi, \eta) &= \sum_{j=1}^{N^{ip}} \Phi_j(\xi, \eta) v_j = \mathbf{\Phi}_{ip}^T \mathbf{v}_{ip} \end{aligned} \quad (16)$$

By substituting Eq. (16) in Eq. (4) one obtains

$$c_i p_i + \sum_{ip=1}^{N_p} \left\{ \iint_{S_{ip}} q_i^* \mathbf{\Phi}_{ip}^T dS \right\} \mathbf{p}_{ip} = \sum_{ip=1}^{N_p} \left\{ \iint_{S_{ip}} p_i^* \mathbf{\Phi}_{ip}^T dS \right\} \mathbf{v}_{ip} \quad (17)$$

Equation (17) can be written for each node “ i ” that belongs to the “ ip ”-th patch out of the total N_p patches, as follows

$$c_i p_i + \sum_{ip=1}^{N_p} \left\{ \int_{S_{ip}} q_i^* \mathbf{\Phi}_{ip}^T(\xi, \eta) |G(\xi, \eta)| d\xi d\eta \right\} \mathbf{p}_{ip} = \sum_{ip=1}^{N_p} \left\{ \int_{\Gamma_{ip}} p_i^* \mathbf{\Phi}_{ip}^T(\xi, \eta) |G(\xi, \eta)| d\xi d\eta \right\} \mathbf{v}_{ip} \quad (18)$$

where the Jacobian is given by

$$\begin{aligned} |G| &= (g_1^2 + g_2^2 + g_3^2)^{1/2} \\ g_1 &= \frac{\partial x_2}{\partial \xi} \frac{\partial x_3}{\partial \eta} - \frac{\partial x_2}{\partial \eta} \frac{\partial x_3}{\partial \xi}, \quad g_2 = \frac{\partial x_1}{\partial \xi} \frac{\partial x_3}{\partial \eta} - \frac{\partial x_1}{\partial \eta} \frac{\partial x_3}{\partial \xi}, \quad g_3 = \frac{\partial x_1}{\partial \xi} \frac{\partial x_2}{\partial \eta} - \frac{\partial x_1}{\partial \eta} \frac{\partial x_2}{\partial \xi} \end{aligned} \quad (19)$$

Now, for the purposes of the numerical integration only, the patch is divided into $N_\xi \times N_\eta$ cells where a second set of normalized co-ordinates ($-1 \leq \xi', \eta' \leq 1$) is introduced, as shown in Figure 2. So, the term $|G(\xi, \eta)| d\xi d\eta$

in Eq. (13) is replaced by $|G(\xi, \eta) \cdot G'(\xi', \eta')| d\xi' d\eta'$, which requires a trivial (e.g., 2×2 , 3×3 , 4×4) Gaussian quadrature.

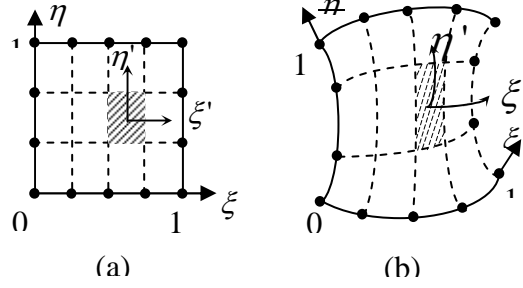


Figure 2. (a) Unit reference and (b) Real patch geometry.

So, the final algebraic system obtains the form

$$\mathbf{C}\mathbf{P} + \sum_{ip=1}^{N_p} \mathbf{H}^{ip} \mathbf{P}^{ip} = \sum_{ip=1}^{N_p} \mathbf{G}^{ip} \mathbf{V}^{ip} \quad (20)$$

where \mathbf{P} is the pressure vector of all nodes on the boundary of the surface (along the patch edges), \mathbf{P}^{ip} and \mathbf{V}^{ip} are pressure and velocity vectors referring to the ip -th patch. Also, the matrices \mathbf{H}^{ip} and \mathbf{G}^{ip} are of order $N_n \times N^{ip}$, where N_n is the number all nodes of the whole surface S and N^{ip} is the number of the ip -th patch. The elements h_{ij}^{ip} and g_{ij}^{ip} of the latter matrices are scalars and relate the i -th geometrical node of the surface S with the j -th node of the ip -th patch. The \mathbf{C} -matrix is a diagonal one of order $N_n \times N_n$.

It is here reminded that apart of the particular case of an ideal smooth boundary, in most cases the number of the geometry nodes is smaller than the number N_m of traction points [4]. So, Eq. (15) finally becomes

$$\mathbf{C}\mathbf{P} + \mathbf{H}\mathbf{P} = \mathbf{G}\mathbf{V} \quad (21)$$

where

- \mathbf{C} : diagonal matrix ($N_n \times N_n$)
- \mathbf{P} : pressure vector ($N_n \times 1$)
- \mathbf{V} : velocity vector ($N_m \times 1$)
- $\hat{\mathbf{H}}$: total pressure–influence matrix ($N_n \times N_n$)
- \mathbf{G} : total velocity–influence matrix ($N_n \times N_m$)

Again, the final pressure–influence matrix ($\hat{\mathbf{H}}$) is square while the velocity–influence one (\mathbf{G}) will be, in general, nonsquare possessing more columns than rows.

With respect to the diagonal terms of the matrix $\mathbf{H} = \mathbf{C} + \hat{\mathbf{H}}$, these can be easily calculated as in the conventional BEM [5]. In this work, no special attention was given to the singular g_{ii} -terms.

3.2 Fictitious eigenvalues

As it was mentioned in the introduction, the BEM solution of exterior acoustic problems with Neumann boundary conditions becomes singular when approaching the eigenvalues of the associated interior Dirichlet problems. In order to circumvent this shortcoming, several remedies have been proposed. In this paper we shall deal with two of them: (a) Least-Squares (LSQ): CHIEF and (b) Lagrange-Multiplier (LM). For more details, one can consult Reference [5]. Both LSQ and LM require the use of a few points inside the surface S , that is inside the volume \bar{V} . For these internal points, additional integral equations are written and are considered in the system of N boundary equations.

I. Lagrange-Multiplier formulation (LM)

Each of the additional integral equations are added to *all* boundary integral equations using a constant Lagrange multiplier. So, the final equations system remains a $N \times N$ system without essential computational cost. More details may be found in Reference [6].

II. Least-Squares formulation (LSQ)

The additional integral equations increase the number of the involved equations and lead to a non-square system. Then, both sides are multiplied on the left by either the transpose (LSQ) or the conjugate transpose (LSQ-Conj) matrix. Obviously, for a large system this procedure seems to be a time-consuming task. However, this “time-consuming” transpose-matrix concept is only for textbooks, while real industrial problems are always solved by a QR-decomposition least-squares solver (which can be found in LINPACK [8], LAPACK [9], etc.). In this way, the increase in the solver time is almost negligible when compared to the regular QR-decomposition for a square matrix. In its initial formulation, this technique is named *Combined Helmholtz Integral Equation Formulation* (CHIEF) [10].

4 EXAMPLES

The efficiency of the proposed method will be elucidated by a typical test problem that refers to the sound radiation due to a monopole at the center of a cube of unit edges. Throughout the six surfaces of the cube, the boundary conditions were taken as the *exact* velocities due to this monopole [5,6]. The exact solution for the acoustic pressure at a distance r from the center of the cube is given by ([12,p.365]; [3, p.311]):

$$p(r) = \frac{a}{r} U_a \frac{jz_0 ka}{1 + jka} e^{-jk(r-a)} \quad (22)$$

where U_a is the normal velocity on the sphere at $r = a$, z_0 is the acoustic impedance ($z_0 = \rho c$) and k is the wavenumber.

The meshes applied to this study are shown in Figure 3. Results will be presented at corner, mid-edge and mid-surface points, using three (32 nodes) and four subdivisions (44 nodes) of the twelve edges of the cube and two different formulations: CHIEF (LSQ: least-squares) and LM (Lagrange-multiplier). With respect to the formulations the interested reader may consult Ref.[5].

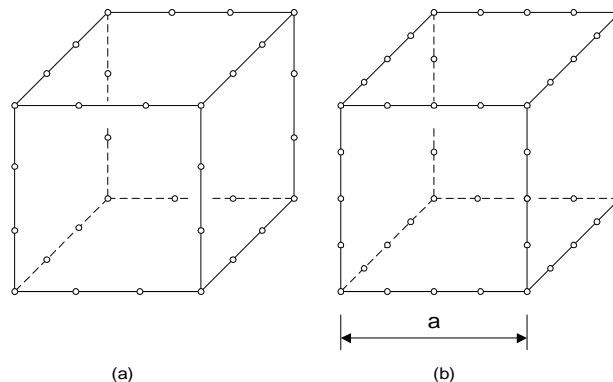


Figure 3. Different discretizations of a vibrating cube using (a) 32 and (b) 44 nodes.

For the fine mesh, results are presented in Figure 4, where the Coons-patch BEM solution using both formulations (LM, LSQ) is very close to the exact solution, in particular for the real part of the acoustic pressure.

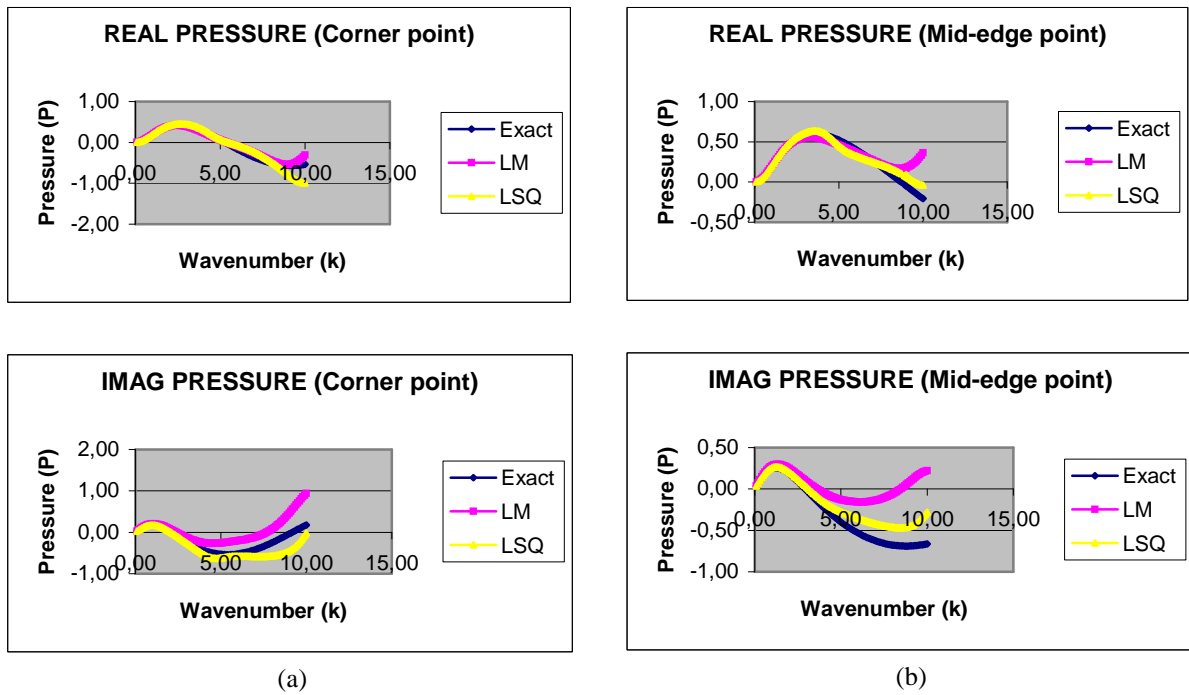


Figure 4. BEM solution using different formulations at a (a) corner point and (b) mid-edge point.

Now, results are presented in Figure 5, for the mid-surface point ($x=0.5, y=0.5, z=1.0$). It can be noticed that the Coons-patch BEM solution oscillates around the curve of exact values but a *very similar* deviation was also observed using conventional boundary elements [6].

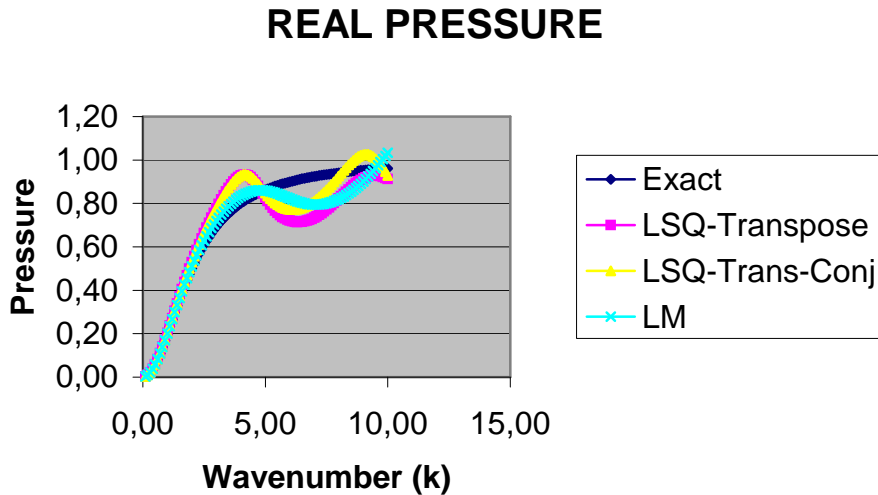


Figure 5. BEM solution using different formulations (mid-surface point)

Finally, Figure 6 illustrates results obtained for the coarse mesh. There, one can notice that both LSQ techniques lead to very similar results, which are slightly better than those obtained through the LM technique.

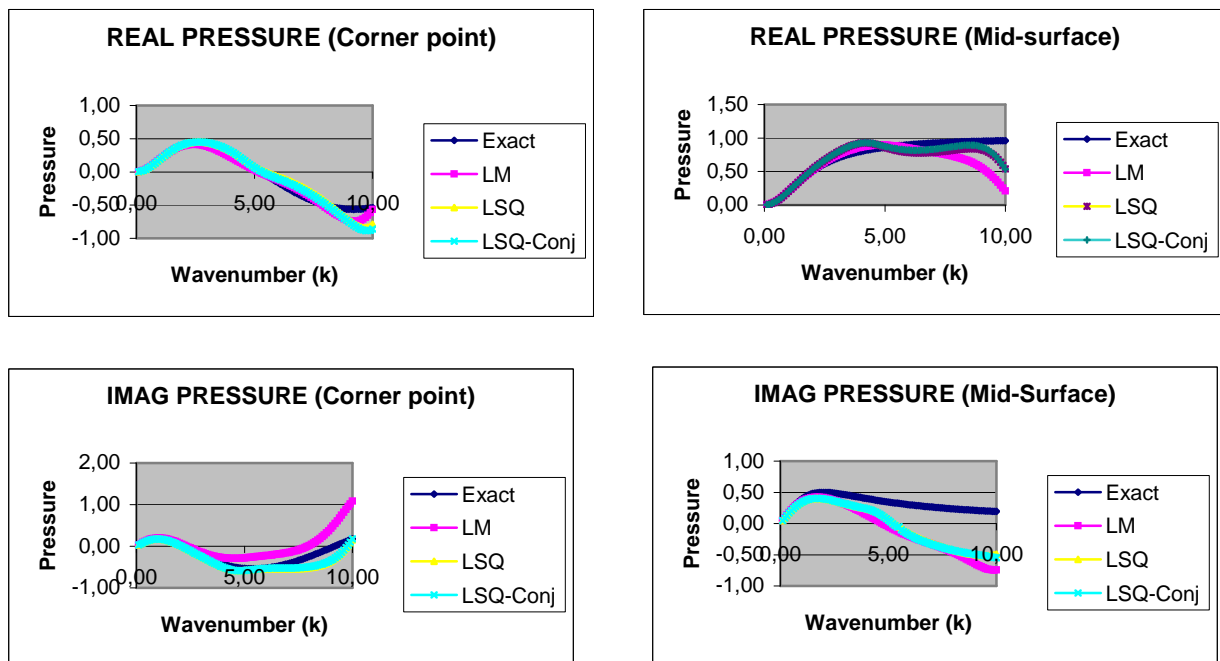


Figure 6. Calculated pressure at two characteristic nodes of a vibrating cube (32 nodes).

5 CONCLUSIONS

It was shown that it is possible to accurately solve sound radiation problems using the BEM in conjunction with large patches, where Coons interpolation is applied. A characteristic of the proposed method is that it leads to reliable results even for a few number of boundary nodes. Moreover, a small increase in accuracy appears when increasing the number of boundary nodes and/or the number of integration points per cell.

The criterion of choosing the patches is related to their geometrical smoothness as well as to the absence of any abrupt changes in the boundary conditions.

Finally, it should be mentioned that in all examples of this paper, the boundary is composed of six discrete patches, which constitute a generalized curvilinear paralleloid. This paralleloid was analyzed by using only its twelve edges. Again, only the boundary data, which are absolutely necessary for the development of the CAD (geometry) model, were involved in the analysis. In this sense, the proposed method seems to “marry” CAD with CAE.

REFERENCES

- [1] Casale M.S., Bobrow J.E. (1989), “The analysis of solids without mesh generation using trimmed patch boundary elements”, *Engineering with Computers*, Vol. 5, pp. 249-257.
- [2] Tzanakis C. (1991), *Elastostatic analysis of three-dimensional structures using large boundary elements based on Coons interpolation*, Diploma Thesis, National Technical University of Athens, (in Greek). Supervisor: C.G.Provatidis.
- [3] Provatidis C.G. (2001), “Stress analysis of 3D solid structures using large boundary elements derived from Coons’ interpolation”, *Proceedings of Greek-ASME Section, September 17-20, Patras*, (CD Proceedings).
- [4] Provatidis C.G. (2002), “Analysis of axisymmetric structures using Coons interpolation”, *Finite Elements in Analysis and Design* (in press).
- [5] Provatidis C.G. and Zafiroopoulos N. (2001), “On the Interior Helmholtz Integral Equation Formulation in sound radiation problems”, *Engineering Analysis with Boundary Elements*, Vol. 26, pp. 29-40.
- [6] Provatidis C.G. (1999), “Improving the BEM analysis in sound radiation problems”, *Proceedings 3rd National Congress on Computational Mechanics, Volos, 24-26 June*, Vol. II, pp. 545-552.
- [7] Provatidis C.G., Kanarachos A.E. (2001), “Performance of a macro-FEM approach using global interpolation (Coons’) functions in axisymmetric potential problems”, *Computers & Structures*, Vol. 79, pp. 1769-1779.
- [8] Dongarra J.J., Bunch J.R., Moler C.B., Stewart G.W. (1979), *LINPACK User’s Guide*, SIAM.
- [9] Anderson E, Bai Z, Bischof C, Blackford S, Demmel J, Dongarra J, Du Croz J, Greenbaum A, Hammarling S, McKenney A, Sorensen D. (1999), *LAPACK User’s Guide*, 3rd edition. SIAM.
- [10] Schenck HA (1968), “Improved Integral Formulation for Acoustic Radiation Problems”, *J Acoust Soc Am*, Vol. 44(1), pp. 41-58.
- [11] Coons, S.A., *Surfaces for computer aided design of space form*, Project MAC, MIT (1964), revised for MAC-TR-41. Springfield, VA, U.S.A.: Available by CFSTI, Sills Building, 5285 Port Royal Road, 1967.